Journal of Power Sources 193 (2009) 691–698

Contents lists available at ScienceDirect

Journal of Power Sources

journal homepage: www.elsevier.com/locate/jpowsour

Experimental evaluation of CO poisoning on the performance of a high temperature proton exchange membrane fuel cell

Susanta K. Das*, Antonio Reis, K.J. Berry

Department of Mechanical Engineering, Center for Fuel Cell Systems and Powertrain Integrations, Kettering University, 1700W. Third Avenue, Flint, MI 48504, USA

ARTICLE INFO

Article history:
Received 26 February 2009
Received in revised form 13 April 2009
Accepted 15 April 2009
Available online 23 April 2009

Keywords:
High temperature PEM
Fuel cell
CO poisoning
Experimental
Performance

ABSTRACT

We experimentally studied a high temperature proton exchange membrane (PEM) fuel cell to investigate the effects of CO poisoning at different temperatures. The effects of temperature, for various percentages of CO mixed with anode hydrogen stream, on the current–voltage characteristics of the fuel cell are investigated. The results show that at low temperature, the fuel cell performance degraded significantly with higher CO percentage (i.e., 5% CO) in the anode hydrogen stream compared to the high temperature. A detailed electrochemical analysis regarding CO coverage on electrode surface is presented which indicates that electrochemical oxidation is favorable at high temperature. A cell diagnostic test shows that both 2% CO and 5% CO can be tolerated equally at low current density (<0.3 A cm^{-2}) with high cell voltage (>0.5 V) at 180 °C without any cell performance loss. At high temperature, both 2% CO and 5% CO can be tolerated at higher current density (>0.5 A cm^{-2}) with moderate cell voltage (0.2–0.5 V) when the cell voltage loss within 0.03–0.05 V would be acceptable. The surface coverage of platinum catalyst by CO at low temperature is very high compared to high temperature. Results suggest that the PEM fuel cell operating at 180 °C or above, the reformate gas with higher CO percentage (i.e., 2–5%) can be fed to the cell directly from the fuel processor.

© 2009 Elsevier B.V. All rights reserved.

1. Introduction

High efficiency, low or zero greenhouse gas emission, portability, and high power density of polymer electrolyte membrane fuel cells (PEMFCs), have attracted much attention as an alternative power source for electric vehicles (EV), auxiliary power unit (APU), portable energy sources or a residential cogeneration power system [1–2]. So far, experimental results and real-world applications of PEMFCs [3–4] revealed that these perform best on pure hydrogen (H_2) as an anode input gas. But for many applications, especially mobile, due to lack of availability of refueling infrastructure and impractical storage techniques pure hydrogen is not yet a viable option [1–2]. Pure hydrogen as an anode gas source for PEMFCs, at present, has a number of formidable limitations [1–2]. One of the major limitations is onboard hydrogen storage. The refueling of a vehicle using hydrogen would be slow, and the major storage schemes of compressed hydrogen, cryogenic hydrogen, and metal hydride adsorption each have significant disadvantages [3–5]. These onboard storage issues are escalated by the lack of infrastructure for hydrogen distribution [2]. As a viable alternative of carrying pure hydrogen, onboard hydrogen generation by reforming hydrocarbons such as natural gas, gasoline or alcohol fuels would be an obvious choice [1–2]. Besides hydrogen and carbon dioxide, the reformate gases contain a small amount of carbon monoxide (CO). Since conventional PEMFCs operate at around 80 °C, at this temperature CO content as low as 10–20 ppm in the hydrogen gas feed results in a significant loss in cell performance due to CO poisoning of the electrodes platinum (Pt) catalyst [1,5–6]. Therefore a strict purification of the reformate gas is necessary in order to reduce CO level down to 10 ppm by means of the water–gas shift reaction, preferential oxidation, membrane separation, or methanation [5–7] which requires considerable effort for additional fuel processing and thus ultimately increases system complexity and cost.

It is well known from a thermodynamic analysis that adsorption of CO on Pt is associated with a high negative entropy, indicating that adsorption is strongly favored at low temperatures, and disfavored at high temperatures [5–7]. Oxidation of hydrogen on the anodic platinum catalyst is known to take place in two different steps i.e., dissociative chemisorption and electrochemical oxidation [6–7]. The dissociative chemisorption of a hydrogen molecule requires two free adjacent sites of the platinum surface atoms. On the other hand, the electrochemical oxidations of the chemically adsorbed hydrogen atoms produce two free platinum sites, two hydrogen ions, and two electrons [6–8]. Hence, the increased tolerance to CO is related to the thermodynamics of adsorption of CO and H_2 on Pt [6–8]. Adsorption of both CO and H_2 on platinum catalyst surfaces is mostly comparable to Langmuirian in nature [6–7].

* Corresponding author. Tel.: +1 810 762 9916; fax: +1 810 762 7860.
E-mail address: sdas@kettering.edu (S.K. Das).

0378-7753/$ – see front matter © 2009 Elsevier B.V. All rights reserved.
doi:10.1016/j.jpowsour.2009.04.021

Nomenclature

A	ampere
A_0	Tafel slope
B_0	mass transfer overvoltage constant
CO	carbon monoxide
E_0	open circuit voltage
H_2	hydrogen
Pt	platinum
r	interaction parameter
R	ideal gas constant
T	temperature
V	voltage
vol	volume
W	power (Watt)

subscripts

θ_{CO}	surface coverage of CO
H_2O	water or water vapor
H_3PO_4	phosphoric acid
%	percentage
i_0	exchange current density

Thus, the operation of low temperature proton exchange membrane (PEM) fuel cell requires CO concentrations as low as 5–8 ppm otherwise CO will poison the electrodes catalyst and a significant loss in fuel cell performance is observed [1–2]. However, hydrogen adsorption is less exothermic than CO on Pt, and H_2 adsorption on Pt requires two adsorption sites at higher temperatures, increasing the temperature of fuel cells may lead to a beneficial shift towards higher H_2 coverage at the expense of CO coverage. CO tolerance is dramatically increased thereby up to 50,000 ppm allowing high temperature PEM fuel cells to use lower quality (higher CO concentrations) reformed hydrogen [8–9].

Numerous studies have been attempted in identifying the mechanism of adsorption and oxidation, and the types and the nature of the adsorbed species using Pt based alloys such as PtRu as CO-tolerant electrocatalysts for the oxidation of adsorbed CO [10–14]. It is found that the presence of Ru atoms in the alloys leads to a bifunctional mechanism i.e., through the promotion of water dissociation and then CO oxidation [11–15]. In fuel cell application, it is found that the oxidation of an adsorbed CO monolayer on the electrodes is shifted to more negative potentials as compared to pure Pt, which implies a lower overpotential at the anode and an increase in cell voltages [8–16]. To use platinum based alloys instead of pure platinum as electrocatalysts in PEMFCs operations; durability, effectiveness and performance degradations of electrocatalysts over time are still major concerns [12–17]. Alternative approach of not using platinum based alloys rather than pure platinum in fuel cell applications to mitigate CO poisoning is the addition of 1–4% oxygen into the CO-containing anode feed stream and is referred to as oxygen bleeding or addition of hydrogen peroxide (H_2O_2) into an anode humidifier have been suggested [10–17]. It has been shown that the cell voltages improvements are much greater than the coulombic losses due to the hydrogen consumption; even though the selectivity of the bleed oxygen is poor i.e., the bleed oxygen reacts chemically with CO and consumes hydrogen as well [13–16]. The aim of addition of H_2O_2 into the humidifier of the anode stream is that the vapor of H_2O_2 can be transported from the anode humidifier to the anode where the oxygen atoms will be formed by dissociative chemisorption on the anode catalyst [14–18]. However, studies suggest that H_2O_2 decomposes at the metallic surface of the anode humidifier and the actual mechanism is also by the oxygen bleed effect [12–18].

The literature reviews presented above clearly indicated that the CO poisoning in the PEMFCs operation is a significant barrier to the commercialization of PEMFC technology for almost all forms of industrial applications especially mobile applications such as transportations. Recently, development of temperature resistant polymer membranes, such as the acid-doped polybenzimidazole (PBI) membranes [19–24], open up the opportunity to build high temperature PEMFC which can be fed with lower quality (higher CO concentrations) reformate hydrogen [8–12] directly from the fuel reformer [10–18]. The high operational temperature makes it possible to improve the CO tolerance of PEMFCs at a higher level. Therefore, the present experimental study of an air breathing high temperature PEM fuel cell at steady operating conditions is to investigate the effects of CO poisoning at different temperatures, 120–180 °C, for extended periods of operations. The aim of this study is to judge the effects of changes in the current–voltage characteristics of the fuel cell at different temperatures while using anode gas feeding with different amount of CO concentrations. Experimental data of this type would be very useful in finding design parameters for fuel processor to deliver the reformate gas directly to the high temperature PEM fuel cells from the reformer without further CO removal. The experimental data will also help to develop multi-dimensional mathematical models which can be used for a more detailed analysis of a high temperature fuel cell, especially for the mass transport analysis from the gas flow channels to the reaction zones.

2. Experimental procedures

In this study, we used our state of the art fuel cell test facility equipped with Schatz Energy Research Center's (SERC) multi-stand test bench. The experimental multi-stand test bench consists of four test stations capable of testing single cell/stacks not exceeding 200 W on the first two stations, while the third and fourth stations can test up to 1000 W at differential pressures up to 2 bar. The fourth test station (TS4) was used for this experimental test of CO effects on fuel cell performance. Our experimental test bench integrates total seven support systems. Both the air and hydrogen systems supply air/hydrogen through the mass flow controllers (MFC) at appropriate pressure levels to the test cell. A single computer, with an analog and digital interface controls and monitors the four test stands on the bench simultaneously, and necessary data acquisitions can be performed in setting auto-mode by the computer.

A single test cell, made of graphite plates carved in serpentine configuration gas channels with 45 cm^2 active areas, is used along with phosphoric acid-doped PBI membrane. The PBI membrane was purchased from BASF Fuel Cell GmbH (Frankfurt, Germany). Electrodes were produced at BASF Fuel Cell Inc. (Somerset, NJ, USA) and the membrane electrode assemblies (MEAs) were performed at BASF Fuel Cell GmbH (Frankfurt, Germany) using phosphoric acid-doped PBI-based (Celtec®–P type) membranes. According to the BASF Fuel Cell, in the MEAs, the cathode contains Pt-alloy with 0.75 mg Pt cm^{-2} and the anode contains Pt catalyst with 1 mg Pt cm^{-2} loading. The membrane thickness in the MEA is approximately 50–75 μm. Two aluminum end plates with attached heaters were used to clamp the graphite plates. Fuel and oxidant gases were supplied via mass flow controllers. Three fuels were used: (i) industrial grade pure hydrogen, (ii) a certified gas mixture consisting of 1.99% CO balanced hydrogen and (iii) a certified gas mixture consisting of 4.99% CO balanced hydrogen, to study the effect of CO concentration in the anode fuel stream on the fuel cell performance at different cell temperatures. All three fuels were supplied from compressed gas cylinders and delivered to the test cell using a MKS mass flow controller. Gas mixtures were certified using a gravimetric method by the CO balanced hydrogen supplied company, The

American Gas Group (AGG), 6055 Brent Dr., Toledo, Ohio, USA. The accuracy level of compositions of various gas mixtures containing H_2 and CO is ±2 rel (a unit used for gas mixture quantification by AGG). We set 1.2 fuel stoichiometry with 0.1 slm (standard liter per minute) minimum fuel flow rate at the anode inlet and 2.5 air stoichiometry with 0.3 slm minimal air flow rate at the cathode inlet and atmospheric (ambient) pressure is maintained at the cell outlets (exits). First, we raised the fuel cell temperature from room temperature to 120 °C and supplied industrial grade pure hydrogen to the fuel cell's anode and then allowed the cell to reach equilibrium/steady state i.e., to reach a stable open circuit voltage (OCV). The actual temperature was within 120–122 °C. Polarization curves of the high temperature PEM fuel cell were measured when the cell voltage reached steady state at 120 °C. At the time the polarizations curves were measured, the cell had already operated for over 1000 h. Upon completion of polarization curve, we set the cell to operate at constant current in order to avoid open circuit voltage. We then set the cell temperature to 140 °C, 160 °C and 180 °C, respectively and polarization curves were measured after the cell had reached steady state at each of these temperatures. Upon completion of polarization curves at each temperature, we set the cell to operate at constant current, each time, in order to avoid OCV. We repeated the above procedures for 2% CO and 5% CO gas mixtures for the entire temperature ranges, 120–180 °C, and completed the measurement of polarization curves. It is interesting to note that for the subsequent use of the same experimental setup, any adsorbed CO was purged with N_2 and then with air. The air purging would oxidize any residual CO on the electrode and would raise the OCV of the electrode.

3. Results and discussions

3.1. Cell performance with pure hydrogen

The fuel cell with 45 cm^2 active area was tested under three different fed gas mixtures. Fig. 1 represents the polarization curves for four different temperatures with pure hydrogen feed at anode stream. Solid lines represent the voltage–current relationship (*I–V*) curves and symbols denote the calculated power output as a function of current density at different temperatures. The cell operating voltage–current relationship can be expressed as [1].

$$V = E_0 - iR - A_0 \ln\left(\frac{i}{i_0}\right) + B_0 \ln\left(\frac{i}{i_l}\right) \quad (1)$$

where V is the cell operating voltage, E_0 is the OCV, iR is the Ohmic loss, A_0 is the Tafel slope, i is the current density, i_0 is the exchange current density, i_l is the limiting current density at the electrode which has the lowest limiting current density and B_0 is the constant of mass transfer overvoltage. From Fig. 1, we can see that as temperature increases the polarization curve shifted upward indicating that cell performs better at higher temperature. It implies that fuel oxidation rate is higher, i.e., higher current density, at higher temperature and consequently cell performance improvement is observed at higher temperatures. At higher temperature, performance gain was observed due to the decrease of the oxygen reduction overvoltage. At the lower temperature, open circuit voltage has a greater impact initially on the cell performance. At a specific cell voltage, for example 0.55 V, the current density increases with increasing cell temperature. At 180 °C and atmospheric pressure, a power output of around 0.39 W cm^{-2} is obtained at the cell voltage of 0.49 V with cell current at around 0.8 A cm^{-2}. At 120 °C, however, the power output is only 0.25 W cm^{-2} at the cell voltage of 0.35 V with cell current density at around 0.7 A cm^{-2}. It is observed that cell temperature has a great impact on the performance of high temperature PEM fuel cell.

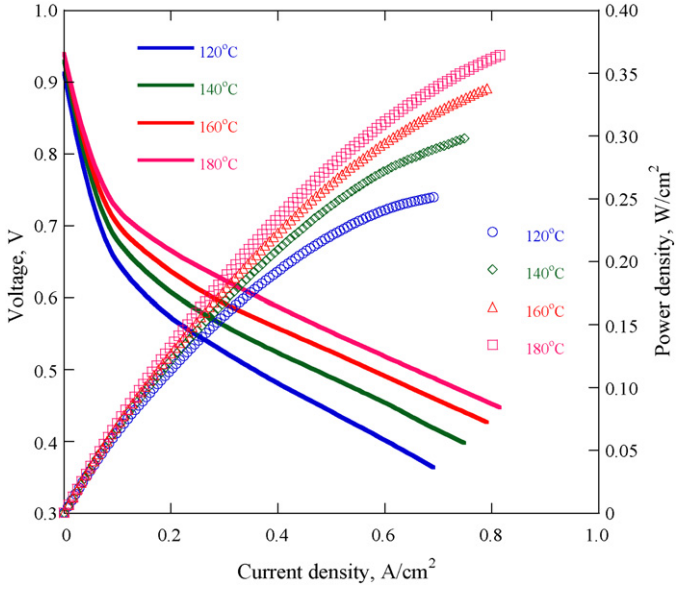

Fig. 1. Polarization obtained experimentally with a PBI-based PEMFC at different temperatures using industry standard pure hydrogen.

3.2. Electrochemical mechanism for pure hydrogen

For the case of adsorption of pure hydrogen on the anode platinum catalyst surfaces, the oxidation of hydrogen takes place in two steps, i.e., dissociative chemisorption occurs first followed by electrochemical oxidation. In the dissociative chemisorption of a hydrogen molecule, two hydrogen atoms are adsorbed chemically by two free adjacent sites of the platinum surface atoms [22].

$$H_2 + PtPt \rightleftharpoons \begin{matrix} H & H \\ | & | \\ Pt & Pt \end{matrix} \quad (2)$$

Next the electrochemical oxidation of the chemically adsorbed hydrogen atoms produces two free platinum sites, two hydrogen ions and two electrons [22]

$$\begin{matrix} H & H \\ | & | \\ Pt & Pt \end{matrix} \rightleftharpoons PtPt + 2H^+ + 2e^- \quad (3)$$

At higher temperature, the oxidation rate of the reactions shown in Eqs. (2) and (3) is higher, which corresponds to a higher current density [23]. The results presented in Fig. 1 complies these electrochemical oxidation and dissociative chemisorption scenarios at higher temperatures.

3.3. Cell performance with CO mixed hydrogen and adsorption of species mechanism

The measured polarization curves with pure hydrogen and the hydrogen containing two different volume (vol) percentage of carbon monoxide (CO) at the temperatures of 140 °C, 160 °C and 180 °C are shown in Fig. 2. For each of the temperatures, CO contents of 0 vol% (0% CO – Pure H_2), 2 vol% (2% CO) and 5 vol% (5% CO) were tested. In Fig. 2, slopes of the current–voltage curves changes significantly at low temperatures (140 °C and 160 °C) with higher CO's (2% CO and 5% CO) compared to high temperature (180 °C). It implies that the higher CO percentage at low temperature poisoned the catalyst layer effectively. From Fig. 2, we can see that, at 140 °C, at the cell voltage of 0.5 V for hydrogen containing 2% CO, the current density decreases from 0.4 A cm^{-2} for pure hydrogen to 0.23 A cm^{-2},

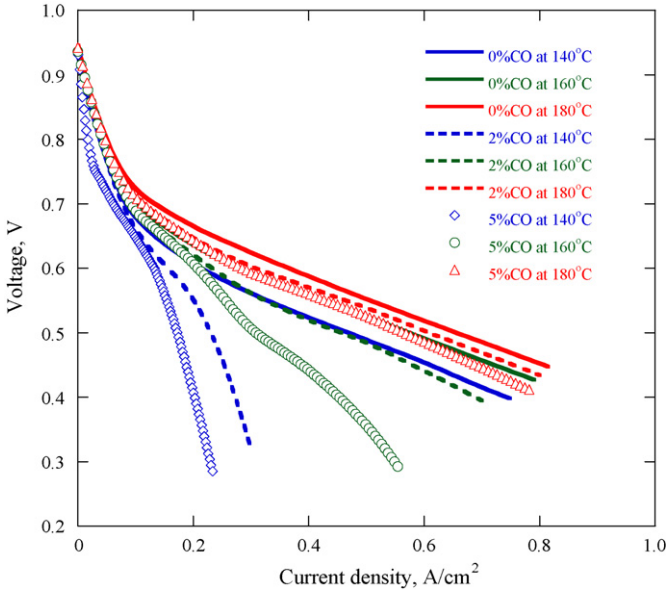

Fig. 2. Polarization curves obtained experimentally with a PBI-based PEMFC with pure hydrogen and 2% CO and 5% CO mixed with pure hydrogen respectively at different temperatures. The % of CO concentrations is indicated in the figure.

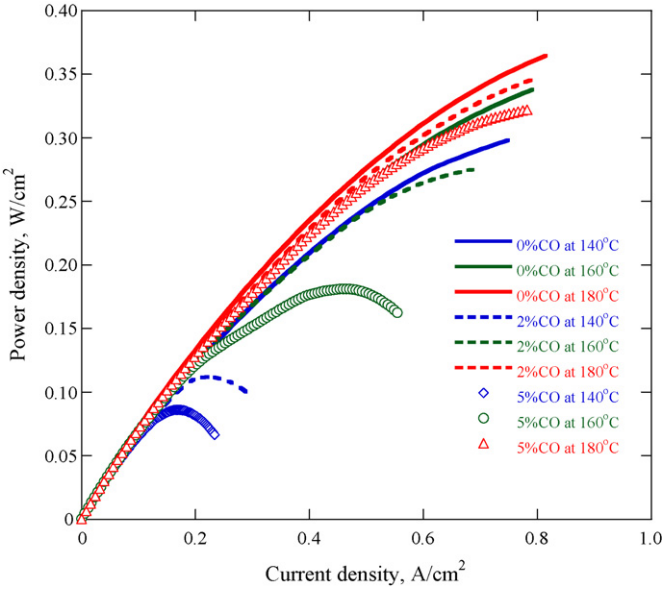

Fig. 3. Power density curves obtained experimentally with a PBI-based PEMFC with pure hydrogen and hydrogen containing different CO vol% at different temperatures. The % of CO concentrations is indicated in the figure.

i.e., current density decreased by 42.5%. For 5% CO, the current density decreases to 0.16 A cm^{-2} at the cell voltage of 0.5 V, i.e., decreased by 60% as compared to pure hydrogen. It reveals that 17.5% performance losses is observed when we increased the CO vol% into the anode feed gas from 2% to 5% at 140 °C. It means that higher CO vol% in the hydrogen stream at low temperature (140 °C) is poisoning fuel cell catalyst effectively. At 160 °C, from Fig. 2, it can be seen that at the cell voltage of 0.5 V, 12.5% performance losses are observed when we increased the CO vol% into the anode feed gas from 2% to 5%. It means that higher temperature enhances fuel cell performance with higher CO vol% in the hydrogen stream. At 180 °C, from Fig. 2, it can be seen that there is no significant performance loss at current densities up to 0.6 A cm^{-2}. For a cell voltage of 0.5 V, approximately 5% performance losses are observed when we increased the CO vol% into the anode feed gas from 2% to 5% at 180 °C. It means that higher CO vol% in the hydrogen stream can be tolerated at higher temperature with minimum degradation of cell performance.

The CO poisoning effect can be better estimated by plotting the power output as a function of the current density. Fig. 3 represents the power density of the cell with different CO percentage in the hydrogen at different temperatures. Red, green and blue solid lines, dashed lines, and symbols represent power density as a function of current density for 0% CO (industrial grade pure hydrogen), 2% CO mixed hydrogen and 5% CO mixed hydrogen at 140 °C, 160 °C and 180 °C respectively. For pure hydrogen, a maximum power density of 0.38 W cm^{-2}, 0.33 W cm^{-2} and 0.27 W cm^{-2} is obtained at current density 0.82 A cm^{-2}, 0.78 A cm^{-2} and 0.75 A cm^{-2} at temperatures 180 °C, 160 °C and 140 °C respectively. When the fuel contains 2% CO and 5% CO the maximum power density decreases to 0.34 W cm^{-2} and 0.31 W cm^{-2} at current density 0.78 A cm^{-2} and 0.77 A cm^{-2}, respectively for the temperature 180 °C. The power density decreases to 0.27 W cm^{-2} and 0.15 W cm^{-2} at current density 0.75 A cm^{-2} and 0.6 A cm^{-2}, respectively for temperature 160 °C whereas power density decreases to 0.1 W cm^{-2} and 0.06 W cm^{-2} at current density 0.36 A cm^{-2} and 0.23 A cm^{-2} respectively for temperature 140 °C when the anode fuel stream contains 2% CO and 5% CO, respectively. From Fig. 3 it appears that the power density of the fuel cell decreases significantly at the lower temperatures (140 °C, 160 °C) as compared to higher temperature (180 °C). When we increased the CO concentration from 2% to 5% in hydrogen stream at different temperatures we found that the power density decreases sharply for higher CO vol% in hydrogen stream at lower temperature which signals that higher CO concentration contaminated anode Pt catalyst very quickly and hence the fuel cell performance degraded profoundly at lower temperatures. The performance losses of high temperature PEM fuel cell due to presence of small amount of CO in the hydrogen stream can be explained by the two competing reactions taking place at the anode. When anode gas stream contains CO, mixed with hydrogen, CO competes with hydrogen for the adsorption sites of platinum. The CO got adsorbed into the platinum sites by two types of bonding modes [22] as shown in Eqs. (4) and (5).

$$H_2 + CO + 3Pt \rightleftharpoons \underset{|}{\overset{CO}{Pt}} + \underset{|}{\overset{H}{2Pt}} \quad \text{(linearly bonded)} \tag{4}$$

$$H_2 + CO + 4Pt \rightleftharpoons \underset{\wedge}{\overset{O}{\overset{\|}{C}}} + \underset{\wedge}{2H} \quad \text{(bridge-bonded)} \tag{5}$$

The adsorption of linearly bonded CO species requires one adsorption site per CO molecules whereas the bridge-bonded CO species requires two adjacent platinum sites [16]. Since adsorption of CO on Pt is strongly favored at low temperatures, and disfavored at higher temperatures [6–14], the cell performance decrease at lower temperature as shown in Figs. 3 and 4. The fuel cell's performance decrease at low temperature may be associated with the adsorption of CO on active Pt sites of the catalyst leading to a blocking of the adsorption and oxidation of hydrogen molecules. Furthermore, by analyzing the anode exhaust gas of a PEMFC using CO mixed with hydrogen, Iwase and Kawatsu [15] showed that with the presence of oxygen containing species, i.e. water or water vapor, CO oxidized to CO_2 at high temperature. Therefore, the desorption of CO can be considered as

$$Pt + H_2O \rightleftharpoons \underset{|}{\overset{OH}{Pt}} + H^+ + e^- \tag{6}$$

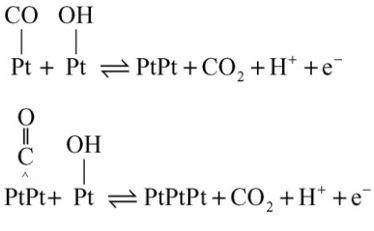

(7)

(8)

The oxidation of CO to CO_2 occurs (see Eqs. (7)–(8)) at potentials where oxygen containing species are formed at Pt surfaces according to Eq. (6). The amount of water or water vapor necessary for the formation of this oxygen containing species on the Pt surfaces may be provided by either by the water vapor in the feed gas or by the water vapor that is present in the proton exchange membrane or the vapor produced inside the fuel cell at high temperature. Thus at high temperature, dissociative chemisorption mechanism of hydrogen molecules can occur further at least on a small fraction of the Pt catalyst surface area free of CO according to Eqs. (7)–(8). Therefore more hydrogen molecules can be bonded by chemisorption on the free Pt surfaces to release more electrons and protons, and consequently the cell performance is improved at high temperature as can be seen from Figs. 3 and 4.

3.4. Comparison of cell performance with pure and CO mixed hydrogen

To compare the CO poisoning effects on the fuel cells performance we plotted the cell voltage loss as a function of current density. The cell voltage loss is calculated by the cell voltage obtained using CO-free hydrogen (industry standard pure hydrogen) minus the voltage obtained using CO-containing hydrogen (different vol% of CO mixed with hydrogen) at different current densities. Fig. 4 represents the cell voltage loss as a function of current density for two different percentage of CO mixed with hydrogen at three different temperatures. In Fig. 4, the solid blue line and blue circles represent voltage loss for 2% CO and 5% CO at 140 °C, respectively, the dashed green line and green diamond symbols represent voltage loss for 2% CO and 5% CO at 160 °C, respectively whereas the red small dashed line and red triangle symbols represent voltage loss for 2% CO and 5% CO at 180 °C, respectively as a function of current density. From Fig. 4, we can see that a small bump-shape appears in the activation loss regime (current density <0.01 A cm^{-2}) for 5% CO at 140 °C. It is because of the fact that poisoning of catalyst is profound for 5% CO at the low temperature, i.e. 140 °C. Because of it, we can see that the voltage drop occurs significantly even in the activation voltage loss regime (current density <0.01 A cm^{-2} – see Fig. 2) for 5% CO at 140 °C. As shown in Fig. 4, the cell voltage loss is very high for 5% CO compared to 2% CO for both at 140 °C and 160 °C at higher current densities. Although the cell voltage loss is approximately equal for 5% CO and 2% CO up to current density 0.23 A cm^{-2} at 180 °C, the cell voltage loss is increasing after current density 0.23 A cm^{-2} for 5% CO compared to 2% CO at 180 °C. If we consider the cell voltage loss within less than 0.05 V, 5% CO and 2% CO in hydrogen can be tolerated at 180 °C up to current densities 0.8 A cm^{-2} as can be seen from Fig. 4. From Fig. 4, if we accept the cell voltage loss within less than 0.07 V, 2% CO in hydrogen can be tolerated at 160 °C at current densities up to 0.64 A cm^{-2} whereas 5% CO in hydrogen can be tolerated at 160 °C at current densities up to 0.57 A cm^{-2} when the cell voltage loss within 0.023 V would be acceptable. At 140 °C, 2% CO and 5% CO can be tolerated at current densities up to 0.25 A cm^{-2} and 0.21 A cm^{-2} respectively when the cell voltage loss of 0.024 V and 0.032 V, respectively would be acceptable. Fig. 5 presents the power loss as a function of current density for 2% CO and 5% CO in the hydrogen stream at temperatures 140 °C, 160 °C and 180 °C. The power loss is calculated by the difference between power obtained using CO-free hydrogen (industry standard pure hydrogen) and CO-containing hydrogen (different vol% of CO mixed with hydrogen) at different current densities. From Fig. 5 we see that 0.07 W cm^{-2} power losses occur for both 2% CO and 5% CO at 140 °C at current densities up to 0.21 A cm^{-2}. At 160 °C, power loss is higher for 5% CO as compared to 2% CO at current density 0.4 A cm^{-2} and 0.57 A cm^{-2}. At 180 °C, power losses are elevated for 5% CO as compared to 2% CO at higher current densities. From the electrochemistry analysis discussed in Eqs. (2)–(8) and the results presented in Figs. 2–6, it is revealed that the cell voltage as well as power loss is apparently a function of the CO content in the anode hydrogen stream, temperature, anode catalyst and current density.

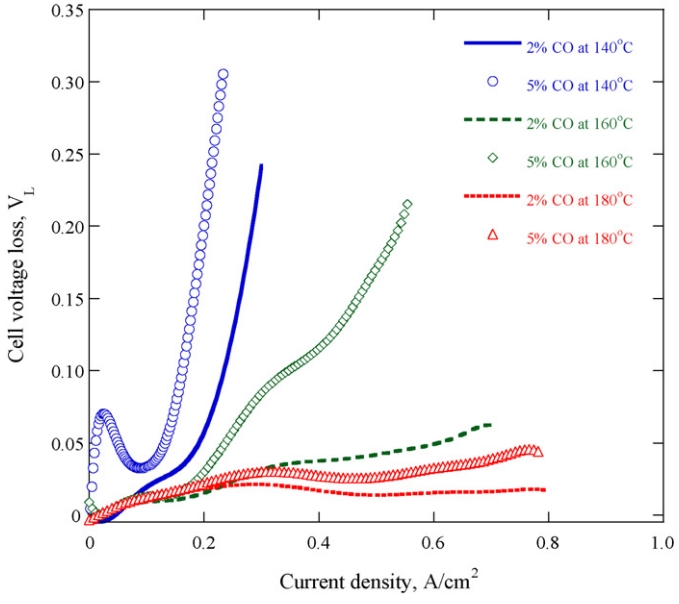

Fig. 4. Cell voltage loss, V_L, obtained experimentally with a PBI-based PEMFC with pure hydrogen and hydrogen containing different CO vol% at different temperatures. The % of CO concentrations is indicated in the figure.

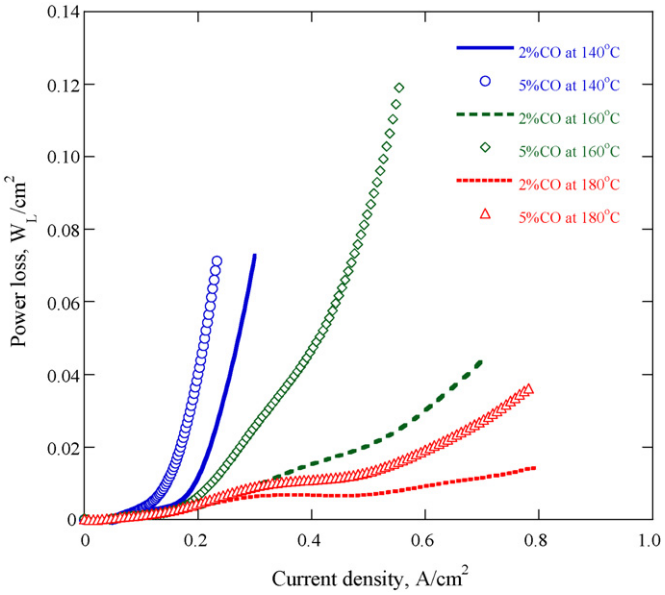

Fig. 5. Cell power loss, W_L (cm^{-2}), obtained experimentally with a PBI-based PEMFC with pure hydrogen and hydrogen containing different CO vol% at different temperatures. The % of CO concentrations is indicated in the figure.

To quantify, more specifically, the effect of CO on the cell performance we tested the cell at two fixed current densities (see Fig. 2 for current–voltage relationship), at 0.2 A cm^{-2} and 0.5 A cm^{-2}, respectively, for 2% CO and 5% CO in the anode hydrogen stream at temperatures ranging between 120 °C and 180 °C. Fig. 6 represents the cell voltage variations as a function of temperatures for 2% CO and 5% CO while the cell was operated at two fixed current densities, at 0.2 A cm^{-2} and 0.5 A cm^{-2}, respectively. For comparison reason, we also tested the cell with pure hydrogen, as a base case, at current density 0.5 A cm^{-2}. In Fig. 6, the dashed green line and blue circles represent the cell voltage for 2% CO and 5% CO at current density 0.2 A cm^{-2}, the dashed red line and pink diamond symbols represent the cell voltage for 2% CO and 5% CO at current density 0.5 A cm^{-2} whereas the black solid line represents the cell voltage at current density 0.5 A cm^{-2} for pure hydrogen as a function of temperature. From Fig. 6, we see that both 2% CO and 5% CO in hydrogen can be tolerated at 180 °C when the cell is operated at current density 0.2 A cm^{-2} with virtually no voltage drop. The cell voltage drop is increasing for 5% CO as the temperature decreasing from 180 °C compared to 2% CO at current density 0.2 A cm^{-2}. From Fig. 6, it is shown that both 2% CO and 5% CO can be tolerated equally if the cell is operated at current density 0.2 A cm^{-2} with cell voltage of 0.65 V. At current density 0.5 A cm^{-2}, the cell voltage drop for 5% CO is more profound than 2% CO as the temperature decreasing from 180 °C compared to the cell voltage for pure hydrogen. From Fig. 6 we see that both 5% CO and 2% CO in hydrogen can be tolerated at 180 °C at current density 0.5 A cm^{-2} when the cell voltage loss within less than 0.03–0.05 V would be acceptable. In brief, from Fig. 6 we see that both 2% CO and 5% CO can be tolerated when the cell operated at low current density, 0.2 A cm^{-2}, and high cell voltage, 0.65 V, at high temperature, 180 °C. On the other hand, when the cell voltage drop within less than 0.05 V would be acceptable compared to the cell voltage for pure hydrogen, both 5% CO and 2% CO in hydrogen can be tolerated at higher current density, 0.5 A cm^{-2}, and lower cell voltage, 0.47 V, at high temperature, 180 °C.

3.5. Electrochemical analysis of CO coverage

According to the electrokinetics [22], the measured current density of a fuel cell comes through hydrogen oxidation, via either

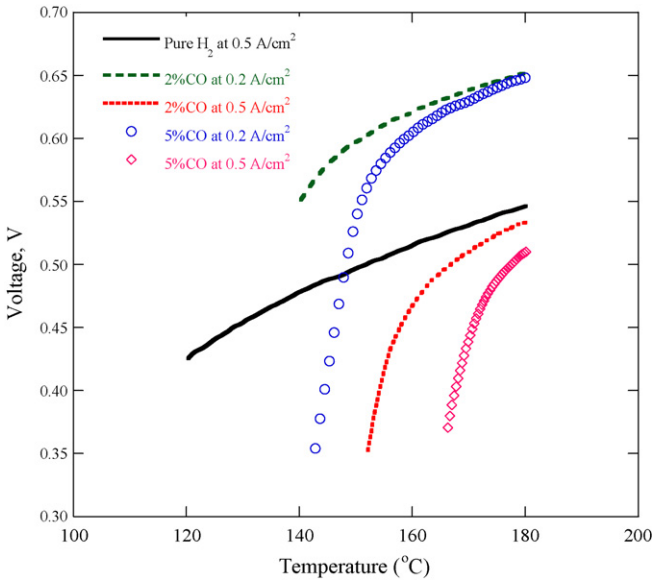

Fig. 6. Variation of cell voltage as a function of temperature at 0.2 A cm^{-2} and 0.5 A cm^{-2}, respectively for both 2% CO and 5% CO mixed with hydrogen. The % of CO concentrations is indicated in the figure.

presence or absence of CO, is directly related to the fraction of unblocked sites, i.e., sites either occupied by hydrogen or available to hydrogen adsorption, $\theta_{\text{unblocked}}$. The surface coverage of platinum (Pt) catalysts by CO, denoted as θ_{CO}, has been determined by a number of researchers [6–15] to characterize the CO poisoning effects. The electrochemical stripping voltammetry and polarization measurements are the two primary tools for estimation of the CO surface coverage. The CO coverage is calculated from the measured cell current as $\theta_{\text{CO}} + \theta_{\text{unblocked}} = 1$. However, this simple additive relationship would not be true in the case of phosphoric acid (H_3PO_4) doped PBI membranes, because of the presence of other possible adsorbed species on the platinum surface. Previous studies [6–17] showed that, under equilibrium conditions, the obtained θ_{CO} values varied in a wide range from 9% for 1% CO in 100% H_3PO_4 at 190 °C to approximately 100% for 10–100 ppm CO in 1 M $HClO_4$ at room temperature (25 °C). For the case of phosphoric acid-doped PBI membranes, the adsorption of the acidic anion ($H_2PO_4^-$) is significant and the adsorption may account for up to 4% of the surface coverage in dilute H_3PO_4 at room temperature for an adsorption potential of 0.1 V [7–16]. If the doped H_3PO_4 in PBI membrane dissolved into water, the anion ($H_2PO_4^-$) adsorption would be appreciably high [8–14]. In addition, as seen in reaction (Eqs. (6)–(8)), the adsorption of hydroxyl ion (OH^-) occurs, especially, at high temperature. Therefore, the calculation of surface coverage of the adsorbed species in H_3PO_4 acid-doped high temperature PEM fuel cell should include at least the following terms.

$$\theta_{\text{CO}} + \theta_{\text{H}_2} + \theta_{\text{H}_2\text{O}} + \theta_{\text{H}_2\text{PO}_4} + \theta_{\text{unblocked}} = 1 \tag{9}$$

where θ represents the fraction of surface sites covered by the indicated species and $\theta_{\text{unblocked}}$ is the available fraction of the free surface sites for any of these adsorbate species. Thus to understand the performance of an acid-doped high temperature PEMFC in the presence of CO in the anode fuel stream, the electrochemistry of CO and hydrogen on the surface of platinum must be understood. Dhar et al. [7] suggested that the adsorption of CO into the platinum surfaces can be presented by the Temkin isotherm, particularly at high temperature:

$$\theta_{\text{CO}} = \frac{-\Delta G_0^0}{r} - \frac{RT}{r}\ln H + \frac{RT}{r}\ln\left(\frac{[\text{CO}]}{\text{H}_2}\right) \tag{10}$$

where G_0^0 is the standard free energy of adsorption, r is the interaction parameter, H is the Henry's law constant for CO solubility in units of atm/(mol per liter). The free energy of adsorption is a function of temperature whereas the interaction parameter is found to be highly dependent on catalyst structure at relatively high temperatures. The CO coverage calculated using Eq. (10) at various temperatures was found to be linear with ln[CO]/[H_2] particularly at low current densities (see Fig. 9 of Dhar et al. [7]).

Thompsett and Cooper [17] proposed that the most appropriate measure for the CO poisoning should be the decrease in fraction of active catalyst surface sites available for the hydrogen oxidation under equilibrium conditions. They defined the measure as the ratio of the active surface site number for the H_2 oxidation in the presence of CO to the total number of available surface sites for the H_2 oxidation in the absence of CO, i.e., the ratio of CO poisoned H_2 oxidation current to the pure H_2 oxidation current, $i_{(\text{CO}+\text{H}_2)}/i_{\text{H}_2}$. Thompsett and Cooper [17] and Igarashi et al. [16] showed that the current ratio would be directly proportional to $(1-\theta_{\text{CO}})$, i.e.,

$$\frac{i_{(\text{CO}+\text{H}_2)}}{i_{\text{H}_2}} = \left(1-\theta_{\text{CO}}\right) \tag{11}$$

Physical interpretation of Eq. (11) is that the current ratio, $i_{(\text{CO}+\text{H}_2)}/i_{\text{H}_2}$, represents the relative activity of the catalyst for hydrogen oxidation in the presence of CO – a value of unity of the ratio indicates no change in the number of active cat-

alyst surface sites for the hydrogen oxidation even in the presence of CO. Vogel et al. [18] used following expressions for the calculation of θ_{CO} from the measured anodic currents

$$\frac{i_{(CO+H_2)}}{i_{H_2}} = \left(1 - \theta_{CO}\right)^2 \quad (12)$$

where $i_{(CO+H_2)}$ and i_{H_2} are the anodic currents due to oxidation of CO mixed with hydrogen and pure hydrogen, respectively at a particular overpotential. Dhar et al. [7] found that the CO coverage obtained using Eq. (12) is in good agreement with their experimental current density. In this study, we calculated the CO coverage, θ_{CO}, using both Eqs. (11) and (12) to judge the relative activity of anode catalyst for hydrogen oxidation. It is interesting to note that a comparative evaluations following [19], accounting for H_2 and CO adsorption features on anode catalytic sites, could be performed by CO stripping voltammetry. Fig. 7 represents the surface coverage of platinum (Pt) catalyst by CO, θ_{CO}, calculated using Eqs. (11) and (12) as a function of temperatures. The blue dashed lines and red dotted lines represent the θ_{CO} calculation using Eqs. (11) and (12), respectively for 2% CO mixed hydrogen fuel whereas the blue solid line masked with open diamond symbol and the red solid line masked with solid circle represent the θ_{CO} calculation using Eqs. (11) and (12), respectively for 5% CO mixed hydrogen fuel. For θ_{CO} calculation presented in Fig. 7, a cell voltage of 0.52 V is chosen for the calculation of $i_{(CO+H_2)}/i_{H_2}$ from the polarization curves with pure hydrogen and hydrogen mixed with CO presented in Fig. 2. From Fig. 7 we see that the surface coverage of platinum (Pt) catalyst by CO for both 2% CO and 5% CO mixed with hydrogen, determined by both Eqs. (11) and (12), is higher around 0.25–0.6 at low temperature, 140 °C, and very low around 0.14–0.012 at high temperature, 180 °C. Physically it means that at low temperature more platinum catalyst sites are occupied by the CO than the platinum catalyst sites occupied by the CO at high temperature. It implies that the free platinum sites for hydrogen adsorption at low temperature is limited compared to the free platinum sites for hydrogen adsorption at high temperature. Thus, due to availability of free platinum sites for hydrogen adsorption, it is reasonable to believe that we observed decreased cell performance for both 2% CO and 5% CO mixed hydrogen fuel at low temperature compared to high cell performance at high temperature for both 2% CO and 5% CO mixed hydrogen fuel as can be seen from Fig. 2. Furthermore, from Fig. 7, we see that the slope of the CO surface coverage curves, determined using Eqs. (11) and (12) for both 2% CO and 5% CO, is decreasing at increasing temperatures. The decrease of the slope of the CO coverage curves with increasing temperature indicates the temperature dependence of the CO poisoning effect on fuel cell performance. One possible explanation for high cell performance at high temperature for both 2% CO and 5% CO mixed with anodic hydrogen fuel stream could be that the electrochemical oxidation mechanism occurs much faster at high temperature especially in the presence of water vapor or membrane water content as can be seen from the electrochemical reactions given in Eqs. (2)–(8). The water vapor content in anode fuel or back diffusion via the membrane or the evaporation of product water at high temperature is a good source of water or water vapor. Since the recovery of free platinum catalyst sites proceeds via water adsorption (see Eq. (7) and (8)), the water content near the anode may affects the recovery rate of free platinum surface sites and consequently enhance the cell performance at high temperature.

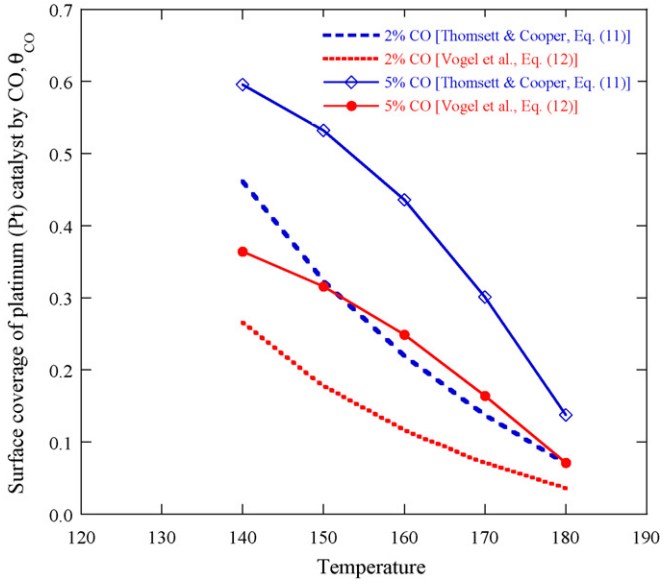

Fig. 7. The surface coverage of platinum (Pt) catalyst by CO, θ_{CO}, calculated using Eqs. (11) and (12) for both 2% CO and 5% CO mixed with hydrogen. The cell voltage is set at 0.52 V for the calculation of θ_{CO}. The % of CO concentrations is indicated in the figure.

4. Conclusion

In this study, using phosphoric acid-doped PBI membrane as electrolyte, the effect of CO poisoning, dispensing through fuel feed at anode stream, on carbon supported platinum catalysts in PEMFC has been investigated in the temperature ranges between 120 °C and 180 °C. It is observed that at low temperature the fuel cell performance degraded significantly with higher CO vol% in the hydrogen stream. At higher temperature, at 180 °C, the fuel cell performance degradation rate is lower compared to low temperature, at 140 °C. The cell performance loss is investigated in terms of cell voltage and power for both 2% CO and 5% CO mixed with hydrogen compared to pure hydrogen at anode fuel stream. A detailed electrochemical analysis based on electrokinetics is presented for possible explanation of cell performance degradation. A cell diagnostic test reveals that both 2% CO and 5% CO can be tolerated equally at high temperature without any cell performance loss at low current density (<0.5 A cm^{-2}) with high cell voltage (>0.55 V) whereas both 2% CO and 5% CO can be tolerated at higher current density (>0.6 A cm^{-2}) with moderate cell voltage (0.45–0.65 V) at high temperature when the cell voltage loss within 0.03–0.05 V would be acceptable. The surface coverage of platinum catalyst by CO is evaluated. The results further show that the surface coverage of platinum catalyst by CO at low temperature is very high compared to high temperature. The overall results suggest that for the case of high temperature PEM fuel cell, operating at near or above 180 °C, the reformate gas with higher CO vol% in the hydrogen stream can be fed to the cell directly from the fuel processor. Experimental data of this type would be very useful to develop design parameters of fuel processor based on reformate hydrocarbons. The high CO tolerance in high temperature PEM fuel cells will make it possible to use the reformate gas directly from the reformer without further CO removal. We are considering the fact that a steam reformer is a consumer of heat and water, and fuel cell stacks are a producer of heat and water. Thus, integration of the fuel cell stack and the reformer is expected to improve the system performance.

Acknowledgement

This work is accomplished under the funding support provided by the U.S. Department of Energy (DOE) grant award number GO86056.

References

[1] J. Larminie, A. Dicks, Fuel cell systems explained, John Willey & Sons Inc., New York, 2000.
[2] J.H. Hirschenhofer, D.B. Stauffer, R.R. Engleman, Fuel Cells-A Handbook (Revision 3), Gilbert/Commonwealth Inc., Reading, 1994.
[3] D.S. Watkins, Research, development and demonstration of solid polymer fuel cell systems, in: L. Blomen, M. Mugerwa (Eds.), In Fuel Cell Systems, Plenum Press, NY, 1993, pp. 493–530.
[4] J. Divisek, H.-F. Oetjen, V. Peinecke, V.M. Schmidt, U. Stimming, Electrochim. Acta 43 (24) (1998) 3811–3815.
[5] J.J. Baschuk, X. Li, Int. J. Energy Res. 25 (2001) 695–713.
[6] H.P. Dhar, L.G. Christner, A.K. Kush, H.C. Maru, J. Electrochem. Soc. 133 (8) (1986) 1574–1582.
[7] H.P. Dhar, L.G. Christner, A.K. Kush, J. Electrochem. Soc. 134 (12) (1987) 3021–3026.
[8] R.J. Bellows, E.P. Marucchi-Soos, B.D. Terence, J. Ind. Eng. Chem. Res. 35 (4) (1996) 1235–1242.
[9] S.M. Aceves, G.D. Berry, J. Energy Resour. Technol. 120 (1998) 137–142.
[10] G. Kohlmayr, P. Stonehart, Electrochim. Acta 18 (2) (1973) 211–223.
[11] P.D. Wilkinson, D. Thompsett, in: O. Savadogo, P.R. Roberge (Eds.), Proceedings of the Second International Symposium on New Materials for Fuel-Cell and Modern Battery Systems, Montreal, Canada, 1997, p. 266.
[12] Q. Li, R. He, G. Ji-An, J.O. Jensen, N.J. Bjerrum, J. Electrochem. Soc. 150 (12) (2003) A1599–A1605.
[13] K.K. Kuo, Principles of Combustion, Wiley and Sons, New York, 1998.
[14] T.A. Zawodzinski, C. Karuppaiah, F. Uribe, S. Gottesfeld, Electrode materials and processes for energy conversion and storage IV, in: S. Srinivasan, J. McBreen, A.C. Khandkar, V.C. Tilak (Eds.), Proceedings of the Electrochemical Society, 97-13, The Electrochemical Society, Inc., Pennington, 1997, pp. 139–146.
[15] M. Iwase, S. Kawatsu, Proton conducting membrane fuel cells I, in: S. Gottesfield, G. Halpert, A. Landgrebe (Eds.), The Electrochemical Society Proceedings Series, PV 95-23, Pennington, NJ, 1995, p. 12.
[16] H. Igarashi, T. Fujino, M. Watanabe, J. Ectectroanal. Chem. 391 (1995) 119.
[17] D. Thompsett, S.J. Cooper, The Electrochemical Society Meeting Abstracts, 94-2, Miami, FL, October 9–14, 1994, p. 948, abstract 607.
[18] W. Vogel, J. Lundquist, P. Ross, P. Stonehart, Electrochim. Acta 20 (1975) 79.
[19] R. Jiang, H.R. Kunz, J.M. Fenton, Electrochim. Acta 51 (2006) 5596.
[20] H.-F. Oetjen, V.M. Schmidt, U. Stimming, F. Trila, J. Electrochem. Soc. 143 (12) (1996) 3838.
[21] C.H. Chen, C.C. Chung, H.H. Lin, Y.Y. Yan, J. Fuel Cell Sci. Technol. 5 (2008) 0145011–0145015.
[22] J.S. Wainright, J.T. Wang, D. Weng, R.F. Savinell, M. Litt, J. Electrochem. Soc. 142 (1995) L121.
[23] J. Wang, Analytical Electrochemistry, third ed., John Wiley and Sons Inc., NY, 2006.
[24] R.M.Q. Mello, E.A. Ticianelli, J. Electrochim. Acta 42 (1997) 1031.